Carbohydrate Research, 84 (1980) 287–295
Elsevier Scientific Publishing Company, Amsterdam – Printed in The Netherlands

SELF-ASSOCIATION OF XANTHAN IN AQUEOUS SOLVENT-SYSTEMS

JEFFREY G. SOUTHWICK, HOOSUNG LEE, ALEXANDER M. JAMIESON, AND JOHN BLACKWELL
Department of Macromolecular Science, Case Western Reserve University, Cleveland, Ohio 44106 (U.S.A.)
(Received June 15th, 1979; accepted for publication in revised form, February 1st, 1980)

ABSTRACT

Quasi-elastic light-scattering studies of the polysaccharide xanthan in aqueous solution reveal the existence of two different structural forms characterized by different values of the translational diffusion coefficient D_t^0. Xanthan dissolved in deionized water yields a value of $D_t^0 = 2.40 \times 10^{-8}$ cm^2/s, provided that the solution is centrifuged or filtered immediately prior to data collection. However, if this solution is allowed to stand for one week, D_t^0 decreases to 1.10×10^{-8} cm^2/s. In contrast, $D_t^0 = 2.75 \times 10^{-8}$ cm^2/s for solutions of xanthan dissolved in 4M urea, and this value does not change with time. These results suggest that xanthan undergoes a self-association in aqueous solution and that this association is inhibited in 4M urea solution, which points to the role of hydrogen bonding in the process. Insertion of our measured values of D_t^0 and the zero-shear intrinsic viscosity into the Flory–Mandelkern equation yields an estimated molecular weight of $\overline{M} = 2.16 \times 10^6$ for xanthan in 4M urea. The aggregation observed in aqueous solutions probably explains the wide variation in molecular weights reported previously for xanthan.

INTRODUCTION

The extracellular polysaccharide produced by the bacterium *Xanthomonas campestris* has become commercially important as xanthan gum[1], especially as an additive in food products. Xanthan gum[2,3] is a polysaccharide possessing extensive short chain-branching; the chemical structure is shown below. The backbone is a cellulose chain [(1→4)-β-D-glucan], and every second backbone-residue has a β-(1→3)-linked trisaccharide side-chain [β-D-mannopyranosyl-(1→4)-(α-D-glucopyranosyluronic acid)-(1→2)-6-*O*-acetyl-β-D-mannopyranosyl]. In addition, the terminal D-mannose residue of the side chain may have a 4,6-linked pyruvic acetal group. The degree of pyruvate substitution is typically 25–50%, and it is uncertain whether the pyruvic acid residues are distributed in blocks along the chain or whether their substitution is random.

A feature of the published literature on xanthan has been the discrepancies in the values reported for the molecular weight. Using classical light-scattering, Dintzis *et al.*[4] obtained a molecular weight of $\overline{M}_w = 2 \times 10^6$ for xanthan in solution

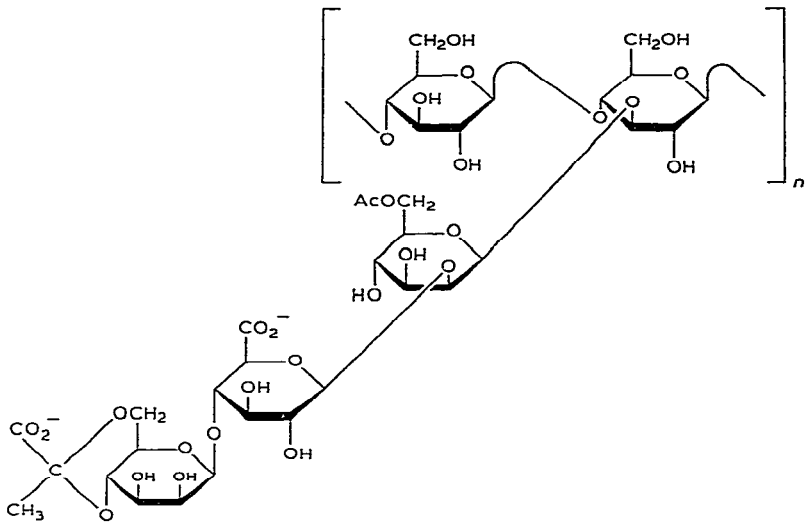

in 4M aqueous urea; the solutions had been maintained at 90° for 1–3 h and then cooled to room temperature before collecting the data. In contrast, urea solutions of two xanthan culture-broths that had undergone no thermal treatment gave molecular weights of $\overline{M}_w = 13 \times 10^6$ and 50×10^6. It was concluded that the thermal treatment led to formation of a true solution in 4M urea, whereas the culture broths are dispersions of aggregated macromolecules. Recently, however, Holzwarth[5] performed band-sedimentation analyses of xanthan solutions (in ~0.75M sodium chloride) in which the macromolecules had been tagged with a fluorescent group. This technique allowed determination of molecular weights at very low concentration; redissolved commercial xanthan was found to have $\overline{M}_w = 14.8 \times 10^6$ ($\overline{M}_w/\overline{M}_n = 2.8$) as compared with $\overline{M}_w = 62 \times 10^6$ ($\overline{M}_w/\overline{M}_n = 2.4$) for the xanthan in native culture-broths. Holzwarth suggested that the culture broths for which Dintzis *et al.* reported high molecular weights were true solutions rather than dispersions, as similar molecular weights were obtained by sedimentation of very dilute solutions[5]. More recently, Rinaudo and Milas[6] performed classical light-scattering studies of xanthan in aqueous sodium chloride solutions, and reported $\overline{M}_w = 2 \times 10^6$, in agreement with the values of Dintzis *et al.*[4] for urea solutions. It is important to note that, in the work of Rinaudo and Milas, the samples were centrifuged for 5 h at 24,000*g* before the data were collected. We are currently investigating the solution properties of xanthan, primarily using quasi-elastic light-scattering. In the course of this work, we have observed a time-dependent aggregation of xanthan in deionized water, which we believe to be the source of the discrepancies in the reported molecular weights.

EXPERIMENTAL

Preparation of solutions. — Samples of xanthan (Kelzan) were obtained from

Kelco Co. and were purified by the method described by Holzwarth[7]. Deionized water for preparation of solutions was prefiltered through 0.1-μm Millipore filters. Sodium azide (0.02%) was added to aqueous solutions to retard bacterial growth. The solutions were adjusted to pH 7 by adding a small quantity of sodium hydroxide and filtered through 0.22-μm Millipore filters, in order to remove residual bacterial cells, and other debris. Concentrations of xanthan were measured by evaporation to dryness after filtration. The urea solutions were maintained for 3 h at 90°, and then cooled to room temperature before collecting the data. Preparations of the solutions before and after filtration and at different intervals thereafter were examined by using a Jeol 100B electron microscope to check for bacterial growth. A small drop of solution was allowed to evaporate on a carbon-coated copper grid, and the residue was lightly shadowed with platinum. Bacterial cells were observed in xanthan samples before filtering, and in samples that had been filtered through 0.45-μm Millipore filters. However, filtration through 0.22-μm Millipore filters gave bacteria-free solutions that remained sterile for over a month.

Quasi-elastic light-scattering. — Laser light-scattering experiments were performed by using a digital photon-correlation spectrometer, and all correlation functions were obtained by collecting the homodyne component of the scattered light. Radiation at 6328 Å from a He–Ne laser was focused on the solution, and the scattered photons were detected by an ITT FW130 phototube with a Pacific Photometrics discriminator/amplifier system. The correlation function was computed by a Honeywell Saicor SA-42 correlation and probability analyzer that was modified to permit digital photon-correlation analysis[8]. Data analysis is straightforward for a monodisperse solution of macromolecules, as the correlation function is an exponential curve of the form:

$$c(\tau) = Ae^{-\Gamma\tau} + B \qquad (1),$$

where $c(\tau)$ is the correlation function, A is a constant, τ is time, B is the baseline, and Γ is the time constant. Γ is determined from the slope of the plot of $\ln c(\tau)$ *vs.* time, and for the homodyne component of the scattered light may be related to the translational diffusion coefficient of a macromolecule by the expression:

$$\Gamma = 2DK^2 \qquad (2),$$

where K is the scattering wave-vector. However, when the sample contains a distribution of molecular weights, a plot of $\ln c(\tau)$ against time exhibits a degree of curvature, and the correlation function cannot be characterized by a unique time-constant. A data-analysis procedure has been applied to polydisperse systems by Brown *et al.*[9] in which a polynomial function is fitted to the points in the plot of $\ln c(\tau)$ against time:

$$\ln|c(\tau)| - B = -\bar{\Gamma}\tau + \frac{1}{2!}\frac{\mu_2}{\bar{\Gamma}^2}(\bar{\Gamma}\tau)^2 - \ldots \qquad (3).$$

The initial slope of the plot ($\bar{\Gamma}$) is now an averaged time-constant and may be related to the z-averaged diffusion coefficient by Eq. *2*. The degree of curvature in the plot

is related to the degree of polydispersity in the sample and is quantified by the parameter $\mu_2/\bar{\Gamma}^2$. We have analyzed the data in this manner, and have also weighted the experimental data-points as suggested by Pusey *et al.*[10].

Centrifugation of samples in the scattering cell prior to data collection is frequently employed to remove small debris from the solution. We have routinely centrifuged xanthan solutions at ~4350*g* for 30 min. However, xanthan solutions in deionized water showed higher translational diffusion coefficients immediately following this centrifugation. This cannot be explained by the sedimentation of debris, as solutions in 4M urea do not show such differences after centrifugation, and solutions in deionized water, which have been filtered through 0.22-μm Millipore filters and centrifuged, exhibit a time-dependent transition of D_t to lower values at room temperature. Therefore, translational diffusion coefficients for xanthan solutions in deionized water were investigated as a function of elapsed time after filtration and centrifugation.

Viscosity measurements. — The zero-shear intrinsic viscosity of xanthan in 4M urea was determined using a 4-bulb, variable-shear capillary viscometer. The xanthan solutions in 4M urea did not exhibit the large decrease in viscosity with increasing shear rate as has been reported for aqueous xanthan solutions[11], and consequently, extrapolation to zero rate of shear is relatively easy. Viscosity measurements were performed at 25 $\pm$0.1°.

RESULTS

Translational diffusion-coefficients normalized to 25° were measured as a function of xanthan concentration in deionized water and 4M urea, and the results

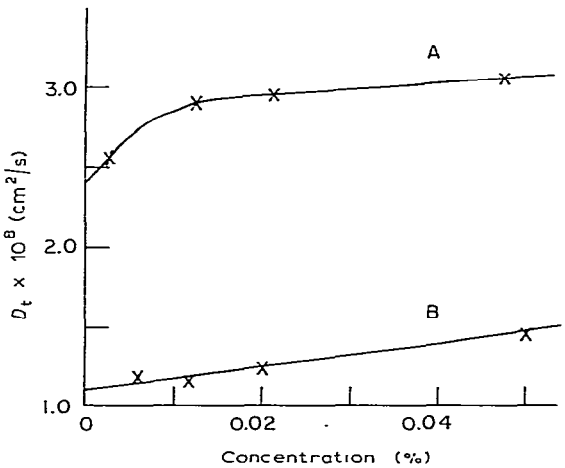

Fig. 1. Translational diffusion-coefficients plotted against concentration for xanthan solutions in deionized water: (A) data collected immediately after centrifuging the solutions at 4350*g* for 30 min; the data were determined at $\theta = 40°$ and are normalized to 25°. (B) equivalent data for the same solutions after one week at room temperature.

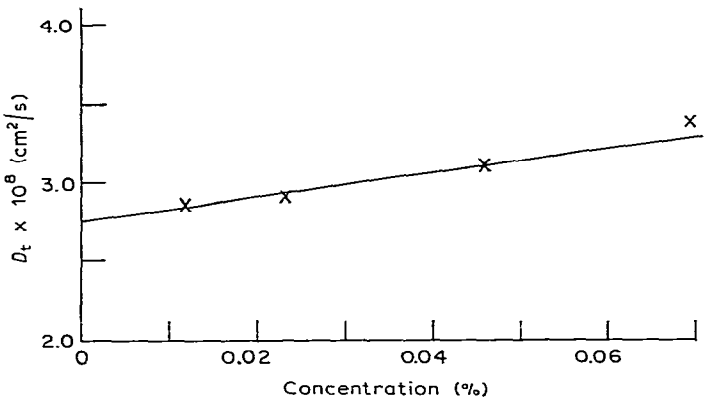

Fig. 2. Plot of diffusion coefficient *vs.* concentration for xanthan solutions in 4M aqueous urea. The data were determined at $\theta = 40°$ and are normalized to 25°. No time-dependence was observed for these solutions.

are given in Figs. 1 and 2, respectively. In this paper we report diffusion coefficients measured in *dilute* solutions. (A solution is defined as dilute when intermolecular overlaps do not affect the translational diffusion of the molecules, that is, $c < c^*$). In a later paper we will describe work at higher concentrations and will discuss these findings in terms of the recent theories of DeGennes[12]. In Fig. 1, curve A shows the diffusion coefficient of xanthan in deionized water solutions that had been filtered through 0.22-μm filters and centrifuged at 4350g for 30 min immediately prior to light-scattering analyses. The diffusion coefficients reported as curve B in Fig. 1 are for similar solutions that had been kept for at least one week at room temperature before collecting the data. It is clear that solutions of xanthan in deionized water gave different diffusion coefficients, depending on whether the data were collected immediately after filtration and centrifugation or the solutions were allowed to stand. If the aged solutions were then filtered and centrifuged, the original value was restored. On the other hand, xanthan in 4M urea solution (Fig. 2) gave the same diffusion coefficient irrespective of whether or not the sample was centrifuged just prior to data collection.

The diffusion coefficient for xanthan in aqueous solution measured immediately after centrifugation may be seen (Fig. 1, curve A) to increase linearly up to a concentration of 0.01%, after which there is a more gradual increase; these results are in qualitative agreement with diffusion data reported previously for a different xanthan specimen[13]. The intercept of curve A at zero concentration gives $D_t^0 = 2.40 \times 10^{-8}$ cm²/s. In contrast, curve B in Fig. 1 yields a value of $D_t^0 = 1.10 \times 10^{-8}$ cm²/s for the same solutions examined one week after recording the data shown in curve A. Fig. 2 shows the diffusion data for xanthan solutions in 4M urea; the intercept of the curve yields $D_t^0 = 2.75 \times 10^{-8}$ cm²/s.

The higher value of the diffusion coefficient ($D_t^0 = 2.40 \times 10^{-8}$ cm²/s) for xanthan in deionized water was observed after the solutions had either been filtered

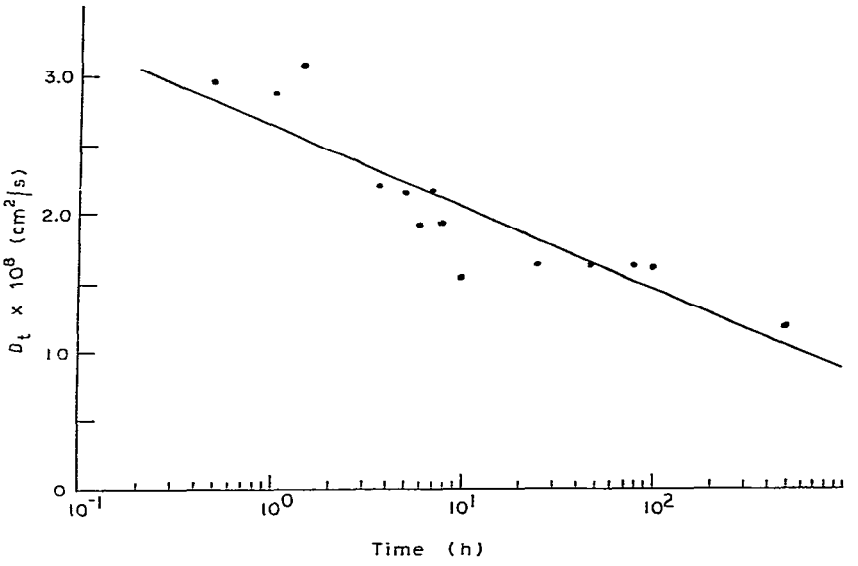

Fig. 3. Translational diffusion coefficients for a 0.02% solution of xanthan in deionized water at 25°, plotted against time.

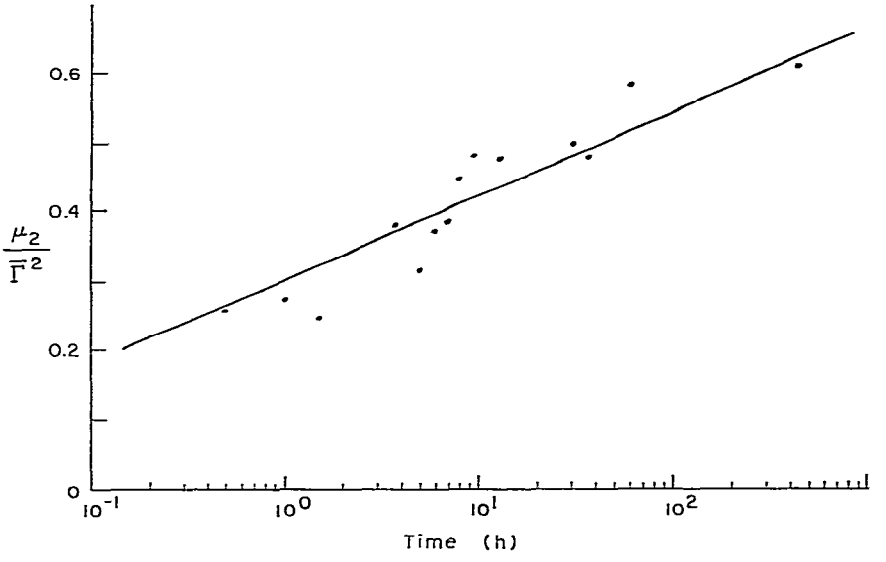

Fig. 4. Second moments ($\mu_2/\bar{\Gamma}^2$) for a 0.02% solution of xanthan in deionized water at 25°, plotted against time.

through 0.22-μm Millipore filters or centrifuged for 30 min at 4350g. Thus the original, xanthan solutions probably contained an equilibrium mixture of aggregated and unaggregated molecules. Centrifugation probably led to sedimentation of the aggregates to the bottom of the scattering cell. In the case of filtration, we measured a

TABLE I

CALCULATION OF $\bar{M}$ FOR XANTHAN IN 4M UREA

Solvent	η_0 *(cp)*	$[\eta]$ *(cc/g)*	D_t^0 *(cm²/s)*	R_h *(nm)*	$\bar{M}$
Urea (4M)	0.9904	2120	2.75×10^{-8}	80	2.16×10^6
Water (centrifuged and filtered)	0.8937		2.40×10^{-8}	110	
(equilibrium)	0.8937		1.10×10^{-8}	222	

concentration loss of no more than 5% after passage through the Millipore filters, and thus either the solutions contained a low proportion of a very large aggregate (sufficient to have a large effect on $\bar{M}$) or, more likely, the shearing forces inherent in the filtration caused disruption of the aggregate.

Fig. 3 shows the time-dependence of D_t for a 0.02% solution of xanthan in deionized water, after the solution had been filtered and centrifuged. The diffusion coefficient is seen to decrease linearly when plotted against log(time), and a constant value is not obtained, even after 500 h. These samples were checked for bacterial growth at various intervals during the 500 h, and since no evidence was seen of bacterial cells, self-association of xanthan molecules is the probable explanation for the observed phenomenon. Fig. 4 shows the $\mu_2/\bar{\Gamma}^2$ values obtained from the same data used to calculate the D_t values plotted in Fig. 4. It may be seen that $\mu_2/\bar{\Gamma}^2$ increases with time; increasing polydispersity with time is suggestive of a time-dependent aggregation phenomenon.

We have used the Stokes–Einstein equation to determine the hydrodynamic radius (R_h) for xanthan in these solutions. In addition, an estimate of the average molecular weight $\bar{M}$ has been determined from the zero shear $[\eta]$ and D_t^0 data, using the Flory–Mandelkern equation[14] for the 4M urea solution. ($\bar{M}$ is expected[15] to occur near the geometric mean of $\bar{M}_w$ and $\bar{M}_z$). The results for these calculations are given in Table I. We could not estimate molecular weights for xanthan in aqueous solution as we were not able to measure an accurate zero-shear intrinsic viscosity for this system.

DISCUSSION

Our experiments suggest that xanthan molecules of molecular weight 2.16×10^6 self-associate in deionized water to form aggregates of very high molecular weight. Urea is a known hydrogen-bond breaker, and the fact that we did not detect the time-dependent aggregation in 4M urea solutions implies a major role for hydrogen bonding in stabilizing the aggregates in water.

An important observation is that our estimated value of the molecular weight for unaggregated xanthan is in agreement with the values previously reported in

the literature by Dintzis *et al.*[4] and by Rinaudo and Milas[6]. The large discrepancies reported in other studies on xanthan probably result from aggregation in some of the xanthan solutions examined. There are now three consistent, independent determinations of the molecular weight for xanthan ($\overline{M} \simeq 2 \times 10^6$), performed on samples obtained from three different sources. It seems likely that it is the species of molecular weight 2×10^6 that is synthesized by the bacterial cell and that this later aggregates and forms the polydisperse distributions of very high molecular weight observed in the culture media. The extent of pyruvate substitution may well be a factor affecting the degree of aggregation.

When aqueous xanthan solutions of low ionic strength are heated, a transition is seen in the hydrodynamic properties of the solution[1,7]. Parallel spectroscopic studies also show a transition with temperature, and it is argued that the increase in temperature disrupts the helical structure of native xanthan, forming a random-coil conformation at higher temperatures[16]. Electron microscopy led Holzwarth to propose that thermal denaturation involves disruption of a multi-stranded helical aggregate consisting of ~40 xanthan chains[17]. The results of this paper are consistent with the foregoing observations and suggest that the thermal denaturation of xanthan involves both disruption of aggregates and a conformational change. We have detected three distinct structural forms of xanthan: a disordered structure having $R_h = 80$ nm; an unaggregated, native, ordered structure having $R_h = 100$ nm; and an aggregate having $R_h = 222$ nm (see Table I). Xanthan probably exists as a disordered coil in the thermally treated, 4M urea solutions, as the hydrodynamic radius is smaller than that determined for the unaggregated xanthan in aqueous solution. It is well established that salt-free solutions of xanthan undergo thermal denaturation at temperatures in the range ~30–50°. Therefore, maintaining 4M urea solutions of xanthan for 3 h at 90° certainly results in denaturation of the ordered form, and when these solutions are cooled the stabilizing hydrogen-bonds of the native structure cannot re-form its structure because of the presence of urea. Based on our observation of time-dependent aggregation in aqueous xanthan solutions, we conclude that thermal denaturation can be interpreted as a concurrent breakdown in aggregate structure and a conformational transition of the xanthan molecule.

The demonstration of time-dependence in the hydrodynamic properties of xanthan solutions suggests that this behavior may also be evident in viscosity measurements. We are currently investigating the effects of ionic strength and temperature on the time-dependent phenomena. In future work we will correlate these hydrodynamic measurements with investigations of the time-dependent character of the shear viscosity in order to gain a further understanding of the rheological role of the xanthan aggregates.

ACKNOWLEDGMENT

We thank Dr. Herbert Morawetz of the Polytechnic Institute of New York for

several enlightening discussions. This work was supported by NSF Grant No. PCM 18631.

REFERENCES

1 A. Jeanes, J. E. Pittsley, and F. R. Senti, *J. Appl. Polym. Sci.*, 5 (1961) 519–526.
2 P. E. Jansson, L. Kenne, and B. Lindberg, *Carbohydr. Res.*, 45 (1975) 275–282.
3 L. D. Melton, L. Mindt, D. A. Rees, and G. R. Sanderson, *Carbohydr. Res.*, 46 (1976) 245–257.
4 F. R. Dintzis, G. E. Babcock, and R. Tobin, *Carbohydr. Res.*, 13 (1970) 257–267.
5 G. Holzwarth, *Carbohydr. Res.*, 66 (1978) 173–186.
6 M. Rinaudo and M. Milas, *Biopolymers*, 17 (1978) 2663–2678.
7 G. Holzwarth, *Biochemistry*, 15 (1976) 4333–4339.
8 H. Lee, A. M. Jamieson, and R. Simha, *Macromolecules*, 12 (1979) 329–332.
9 J. C. Brown, P. N. Pusey, and R. Dietz, *J. Chem. Phys.*, 62 (1975) 1136–1144.
10 P. N. Pusey, D. E. Koppel, D. W. Schaefer, R. D. Camerini-Otero, and S. H. Koenig, *Biochemistry*, 13 (1974) 952–960.
11 P. J. Whitcomb and C. W. Macosko, *J. Rheol.*, 22 (1978) 493–505.
12 P. G. DeGennes, *Macromolecules*, 9 (1976) 587–593.
13 J. G. Southwick, M. E. McDonnell, A. M. Jamieson, and J. Blackwell, *Macromolecules*, 12 (1979) 305–311.
14 L. Mandelkern and P. J. Flory, *J. Chem. Phys.*, 20 (1952) 212–214.
15 M. E. McDonnell and A. M. Jamieson, *J. Appl. Polym. Sci.*, 21 (1977) 3261–3267.
16 E. R. Morris, D. A. Rees, G. Young, M. D. Walkinshaw, and A. Darke, *J. Mol. Biol.*, 110 (1977) 1–16.
17 G. Holzwarth and F. G. Prestridge, *Science*, 197 (1977) 757–759.